The Application of Highly Doped Single-Layer Graphene as the Top Electrodes of Semitransparent Organic Solar Cells

Zhike Liu, Jinhua Li, Zhen-Hua Sun, Guoan Tai, Shu-Ping Lau, and Feng Yan*

Department of Applied Physics and Materials Research Centre, The Hong Kong Polytechnic University, Hong Kong, China

ABSTRACT

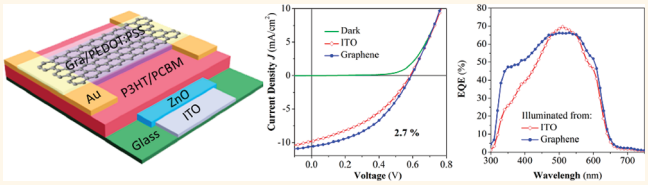

A single-layer graphene film with high conductance and transparency was realized by effective chemical doping. The conductance of single-layer graphene was increased for more than 400% when it was doped with Au nanoparticles and poly(3,4-ethylenedioxythiophene): poly(styrene sulfonic acid). Then semitransparent organic solar cells based on poly(3-hexylthiophene) (P3HT) and phenyl-C61-butyric acid methyl ester (PCBM) were fabricated with single-layer graphene and indium tin oxide (ITO) as the top and bottom electrodes, respectively. The performance of the devices was optimized by tuning the active layer thickness and doping the single-layer graphene electrodes. The maximum efficiency of 2.7% was observed in the devices with the area of 20 mm^2 illuminated from graphene electrode under the AM1.5 solar simulator. It is notable that all of the devices showed higher efficiency from the graphene than ITO side, which was attributed to the better transmittance of the graphene electrodes. In addition, the influence of the active area of the organic solar cell on its photovoltaic performance was studied. We found that, when the active areas increased from 6 to 50 mm^2, the power conversion efficiencies decreased from 3% to 2.3% because of the increased series resistances and the decreased edge effect of the devices.

KEYWORDS: organic solar cell · graphene · PEDOT:PSS · doping · conductance · field effect transistor

Graphene has attracted much attention recently for its fascinating physical properties, including Dirac Fermi behavior,[1,2] high carrier mobility,[3,4] excellent mechanical flexibility and transparency,[3] *etc.* Since indium tin oxide (ITO) becomes more expensive due to limited resources of indium, graphene has been recognized as an important material for transparent electrodes in optoelectronic devices in the future, including solar cells,[5−9] light emission diodes, photo sensors,[10] and transparent thin film transistors.[11] In addition, graphene shows much better mechanical flexibility than ITO and metal electrodes. Therefore it is suitable for the applications in flexible electronics.[5] Recently, graphene has been used as transparent electrodes for both organic and dye-sensitized solar cells in many research groups. However, the research is still at the early stage and the performance of such devices has not been as good as that of the devices with ITO electrodes since the conductivities of graphene electrodes are relatively low.[12−15] For example, Arco *et al.* reported a flexible organic solar cell with a 0.75 mm^2 graphene electrode, which showed a power convention efficiency (PCE) up to 1.3%.[5] Park *et al.* reported organic solar cells with Au-doped graphene electrodes (1.21 mm^2), and the maximum PCE of such device was 1.63%.[7] Wang *et al.* reported an organic solar cell using a lay-by-layer stacked graphene anode (4 mm^2) with a PCE of 2.5%.[9] Nevertheless, we can find that the device performance has been improved by various approaches, such as using stacked multilayer graphene or chemically doped graphene films,[7,9,12] indicating that graphene is a promising material for transparent electrodes of organic solar cells. It is notable that all of the graphene electrodes used in the aforementioned devices were multilayer graphene films. To be a transparent electrode, single-layer graphene is preferred for its better transparency, which will be studied in this paper. Another drawback of the reported organic solar cells with graphene electrodes is the small active area. The biggest area of such devices is only 10 mm^2, which may lead to an overestimation of the PCE due to edge effect.[16] It is reasonable to expect that large area organic solar cells

* Address correspondence to apafyan@polyu.edu.hk.

Received for review November 5, 2011 and accepted December 10, 2011.

Published online December 11, 2011
10.1021/nn204675r

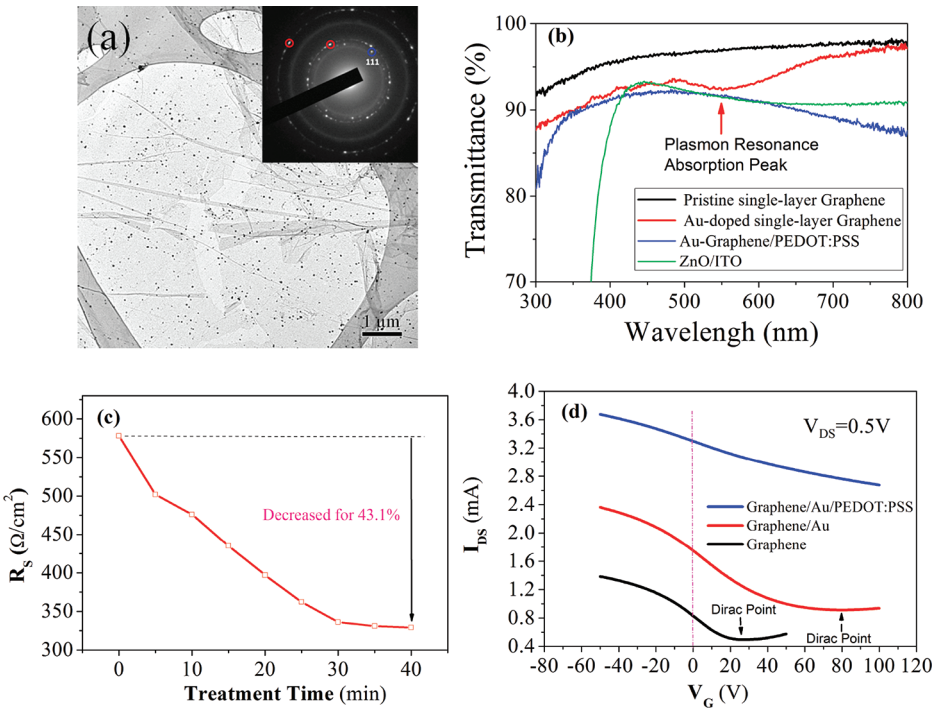

Figure 1. (a) TEM picture of a single-layer graphene film doped with Au nanoparticles. Inset: Diffraction pattern of the Au-doped graphene film. Red and blue circles present the diffraction patterns of graphene and Au, respectively. (b) Light transmittance of single-layer graphene before and after Au doping, Au-doped graphene/PEDOT:PSS, and ZnO/ITO films on glass substrates. (c) Sheet resistance of a single-layer graphene as a function of treatment time in $HAuCl_4$ solution. (d) Transfer characteristics (I_{DS} *vs* V_G) of graphene transistors with different chemical doping. V_{DS} = 0.5 V.

with single layer graphene can be fabricated more conveniently compared with the ones with multilayer graphene that needs to be transferred and stacked for many times.[9]

Besides its use as the bottom electrode for organic solar cells, we find that graphene is an excellent candidate for the top electrode of a semitransparent organic solar cell since large area graphene films can be easily transferred to the top of various substrates by a solution process at room temperature.[17] Semitransparent solar cells are very useful in some special applications, such as power-generating tinted thin films coated on electrical appliances, windows, foldable curtains, buildings, and clothes, *etc.*[18] In such a semitransparent solar cell, transparent electrodes will be used as both cathode and anode. Therefore the device can absorb light from both sides and can be integrated with other solar cells to form tandem devices.[19] However, the efficiency of a semitransparent solar cell is relatively low because the light absorption is lower than that in a normal device which contains a metal electrode that is able to reflect light and increase the light absorption of the active layer. For example, Lunt *et al.* reported a semitransparent organic solar cell with a PCE of 1.3%.[20] Ameri *et al.* showed semitransparent solar cells by using an ITO layer as cathode and a Ag grid as anode, which can be illuminated on both sides with PCE up to 2%.[18] Xia *et al.* reported a infrared transparent polymer solar cell by using carbon nanotube electrodes, and an efficiency up to 2.5% was realized.[21] Huang *et al.* reported a semitransparent solar cell by a laminating process with two ITO electrodes, and the maximum power efficiency of 3.2% was obtained.[22]

In this paper, we report the fabrication of a semitransparent organic solar cell based on poly(3-hexylthiophene) (P3HT) and phenyl-C61-butyric acid methyl ester (PCBM) with a single-layer graphene as top electrode. The devices have been optimized by tuning the active layer thickness and changing the conductance and the work function of single-layer graphene by doping Au nanoparticles and poly(3,4-ethylenedioxythiophene)/poly(styrene sulfonic acid) (PEDOT:PSS) solution. The maximum PCE of the semitransparent solar cell with the active area of 20 mm^2 illuminated from graphene electrode is 2.7%. Then the influence of the active area on the device performance is studied. We find that the PCE of the device decreases from 3% to 2.3% with the increase of the size from 6 to 50 mm^2, which can be attributed to both the increased series resistance and the decreased edge effect of the device.

RESULTS AND DISCUSSION

Large-area single-layer graphene films were synthesized on copper foils with the chemical vapor deposition (CVD) method.[17] Then the graphene films were transferred onto various substrates by coating PMMA layers on the top.[23] A single-layer graphene film after the transfer has been characterized under Raman

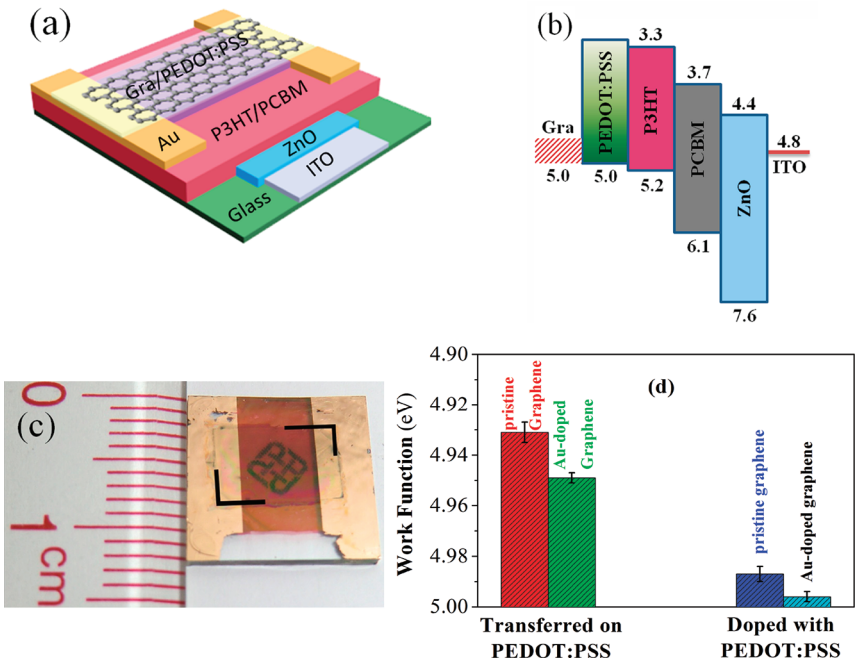

Figure 2. (a) Schematic diagram of a semitransparent organic solar cell with the structure glass/ITO/ZnO/P3HT:PCBM/PEDOT:PSS/graphene; (b) band structure of the organic solar cell;[28,29] (c) semitransparent solar cell with graphene top electrode. The edges of the graphene electrode are indicated by black lines; (d) work functions of graphene/PEDOT:PSS electrodes prepared at different processing conditions.

spectroscopy (see Supporting Information, Figure S1).[17] To increase the conductances of the graphene films, we put the films in $HAuCl_4$ solution for a certain period of time (*i.e.*, treatment time) before they were transferred onto substrates.[12] Figure 1a shows the TEM image of a single layer graphene film after the treatment of $HAuCl_4$. The diffraction pattern in the inset shows that the graphene film is polycrystalline.[24] Lots of Au nanoparticles with the average diameter of 30 nm can be observed on the graphene after the treatment, which has been regarded as p-type doping due to the higher surface potential of Au than that of graphene (*i.e.*, Au particle receive electrons from graphene).[12] Figure 1b shows the transmittance of a graphene on glass substrate before and after the treatment. An absorption peak with a height of about 5% can be observed at the wavelengths around 540 nm, which is due to the surface plasmon resonance absorption of Au nanoparticles.[25] Figure 1c shows the sheet resistance of graphene film as a function of treatment time. One can find that the sheet resistance is decreased by 43% after a treatment longer than 30 min. Further treatment cannot decrease the resistance anymore.

To better understand the doping effect in graphene films, graphene transistors have been fabricated on n^+Si/SiO_2 substrates. Graphene films with or without Au-doping have been transferred on the substrates followed by the deposition of Au source/drain electrodes. The n^+Si substrates were used as the gate electrodes of the transistors. Figure 1d shows the transfer characteristics (I_{DS} *versus* V_G, $V_{DS} = 0.5$ V) of the devices fabricated at different conditions, where I_{DS} is the channel current, V_{DS} is the drain voltage, and V_G is the gate voltage. For the device with a pristine graphene film, the Dirac point is at the gate voltage of about 25 V, indicating p-type doping behavior of the graphene probably due to the absorbed water.[1] The device with Au-doped graphene shows the Dirac point at about 80 V, which means that the graphene with Au nanoparticles receives heavier p-type doping. Here, the doping time of the graphene film in $HAuCl_4$ is 30 min. It is notable that the channel current at zero gate voltage is increased for more than 100% after Au-doping, which corresponds to the decrease of the sheet resistance of graphene for about 50%, being consistent with the results shown in Figure 1c.

To further increase the conductance of the graphene film, we coated a thin PEDOT:PSS layer (~30 nm) on top of the Au-doped graphene film followed by thermal annealing at 120 °C for 20 min in a glovebox. Because a PEDOT:PSS film is p-doped and has a work function (about 5 eV) higher than that of graphene (about 4.6 eV),[12,26,27] electrons will transfer from graphene to PEDOT:PSS film after the coating and thus the graphene film will be doped with holes (*i.e.*, p-type doping). The transfer characteristic of the transistor shows an obvious p-type doping effect by PEDOT:PSS, as shown in Figure 1d. The Dirac point is moved to the gate voltage higher than 100 V, which is out of the detectable range of the device. The channel current is increased for more than 3 times at zero gate voltage compared with that of the pristine device, indicating

that the sheet resistance of the film is decreased for more than 75% after the coating. The contribution of the PEDOT:PSS layer in the conductance of the graphene film is estimated to be less than 3%. Therefore the decrease of the resistance of the graphene film is mainly due to the p-type doping by PEDOT:PSS solution.

To use the p-doped graphene in organic solar cells as top electrodes, we can fabricate the devices with the inverted structure: glass/ITO/ZnO/P3HT:PCBM/PEDOT:PSS/graphene,[22] as shown in Figure 2a. Here, ZnO and PEDOT:PSS act as electron and hole transport layers, respectively.[28] Figure 2b shows the cascaded band structure of the inverted solar cell,[29,30] which is favorable for exciton dissociation and charge transfer to both electrodes.[31] For example, electrons (holes) generated in the active layer can easily move to the ITO cathode (graphene anode) for decreased energy at each interface along this direction. Figure 2c shows a semitransparent organic solar cell with graphene anode on the top. The size of the active area of the solar cell is 5 mm × 4 mm, which is much bigger than the active areas of previously reported organic solar cells with graphene electrodes.[9] It is notable that there are two gold electrodes deposited on both sides of the solar cell, which are used to characterize the sheet resistance of the graphene electrode in the device prepared at different processing conditions.

The organic solar cells were fabricated with solution process as reported before.[31−34] It is notable that graphene electrodes only can be transferred in air. So all of the devices fabricated in air need to have post-annealing at 120 °C for 20 min in the glovebox to remove oxygen and moisture in the active layer, as explained in our previous paper.[32] For each fabrication condition, three identical devices were fabricated and the average PCE was calculated. The device performance was optimized in the following three steps: (1) optimize the thickness of the P3HT:PCBM active layer; (2) dope the graphene electrode with Au; (3) dope the graphene electrode with PEDOT:PSS solution. The ideal thickness of the active layer of an organic solar cell with a metal electrode is about 200 nm, which is a compromise between light absorption and charge transport.[14,32] However, a semitransparent solar cell shows lower light absorption than a normal device and a thicker active layer is thus needed. P3HT:PCBM was dissolved in chlorobenzene with three different concentrations (20:16, 25:20, 30:25 mg/mL) and coated on ITO/ZnO substrates with different thicknesses (200, 308, and 410 nm). Then a PEDOT:PSS layer was coated on the active layer followed by graphene transfer on the PEDOT:PSS film as the top electrode.[20]

The sheet resistance of PEDOT:PSS layer before graphene transfer was measured to be higher than 3 kΩ/□. After graphene transfer, the graphene/PEDOT:PSS electrode has a sheet resistance of 550 Ω/□. After thermal annealing at 120 °C for 20 min, the sheet

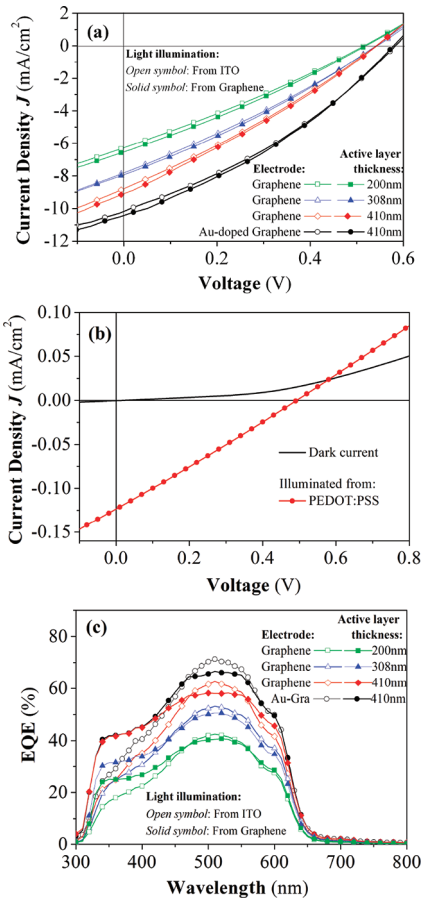

Figure 3. (a) *J*−*V* characteristics (photocurrent density as a function of voltage) measured from two sides of semitransparent organic solar cells with graphene top electrodes and different active layer thicknesses. (b) *J*−*V* characteristics of an organic solar cell with PEDOT:PSS top electrode. The thickness of active layer is 410 nm. (c) External quantum efficiency (EQE) measured from both sides of organic solar cells with graphene top electrodes and different active layer thicknesses. The open and solid symbols correspond to the results characterized from ITO and graphene sides, respectively.

resistance is decreased to 470 Ω/□. This effect may be due to the improved adhesion of graphene on PEDOT:PSS film that leads to p-type doping in graphene. The sheet resistance is slightly increased to 486 Ω/□ after the device is packaged and taken out of the glovebox for measurements. It is notable that the doping effect of PEDOT:PSS on graphene is much weaker when the graphene layer is transferred on solid PEDOT:PSS film compared with the case when the graphene layer is coated with PEDOT:PSS aqueous solution, which is probably due to the poor adhesion of graphene on the PEDOT:PSS layer in the former case.

In addition, the surface potential of the graphene electrodes doped with different conditions have been characterized using scanning Kelvin probe microscopy (SKPM).[35] In each sample, a Au electrode was evaporated on graphene film and the potential difference between graphene and Au film was characterized for three times. Since the work function of Au is 5.0 eV, the work

TABLE 1. Photovoltaic Parameters of Semitransparent Organic Solar Cells with Different Active Layer Thicknesses Characterized from Two Sides

anode	active layer thickness	illumination side	J_{SC} (mA/cm^2)	V_{OC} (V)	R_s (Ωcm^2)	FF (%)	η (%)
graphene	200 nm	ITO	6.27	0.515	59.33	28.1	0.91 ± 0.2
		graphene	6.52	0.520	59.42	28.3	0.96 ± 0.2
graphene	308 nm	ITO	7.80	0.540	48.85	28.7	1.21 ± 0.1
		graphene	7.91	0.542	44.36	29.0	1.25 ± 0.2
graphene	410 nm	ITO	8.78	0.539	39.12	28.9	1.34 ± 0.1
		graphene	9.07	0.542	39.59	28.5	1.40 ± 0.2
Au-doped graphene	410 nm	ITO	10.14	0.578	28.60	33.3	1.95 ± 0.1
		Au-doped graphene	10.40	0.581	27.44	32.8	1.98 ± 0.1
PEDOT:PSS	410 nm	PEDOT:PSS	0.123	0.49	4624	26.5	0.016

functions of the graphene electrodes prepared at different conditions can be decided as shown in Figure 2d. It is notable that the graphene codoped with Au and PEDOT:PSS shows the highest work function.

Figure 3a shows the photocurrent densities as functions of bias voltage ($J-V$) of the organic solar cells with different active layer thicknesses. The devices were illuminated on each side under an AM1.5 solar simulator with the intensity of 100 mW/cm^2. The efficiencies of the devices increase with the increase of active layer thickness due to higher light absorption (see Supporting Information, Figure S2). The maximum efficiency is about 1.4%, corresponding to the thickness of about 410 nm, as shown in Table 1. But the fabrication of a uniform and thicker active layer is technically difficult. Therefore all of the devices in the following experiments have active layer thicknesses of about 410 nm. A control experiment showed that the device with only a PEDOT:PSS top electrode without a graphene layer had an efficiency of ~0.016%, as shown in Figure 3b and Table 1. Therefore the graphene top electrode is the essential part for the organic solar cell. It is notable that all of the devices showed higher efficiency when they were illuminated from graphene than from an ITO electrode. Figure 3c shows external quantum efficiency (EQE) of the devices. One can find that the quantum efficiency of the device illuminated from the ITO side is higher than that from graphene side at the wavelengths around 500 nm. However, it is a different case at short wavelength region below 450 nm. This behavior can be attributed to the lower transmittance of graphene/PEDOT:PSS electrode at around 500 nm while higher transmittance at short wavelengths than that of ITO/ZnO electrode, as shown in Figure 1b. Since the photon energy in the short wavelength region (<400 nm) has the portion of ~6.4% in solar spectrum,[36] higher EQE of the device in this region can induce an evident increase of PCE. Therefore the different efficiencies of the device illuminated on two sides can be attributed to the different light transmittance of front electrodes.

The second step is to improve the conductance of graphene electrode with chemical doping. Graphene film was treated with $HAuCl_4$ solution for 30 min. Then Au-doped graphene film was transferred on PEDOT:PSS layer of organic solar cell and the sheet resistance of the electrode characterized afterward is 305 Ω/□. The resistance is decreased to 284 Ω/□ after a thermal annealing at 120 °C for 20 min and then increased to 293 Ω/□ after packaging. The $J-V$ characteristics and EQE of the device with Au-doped graphene electrode are shown in Figure 3. All of the parameters, including short circuit current (I_{SC}), open circuit voltage (V_{OC}) and fill factor (FF) are improved, as shown in Table 1. The PCEs of the device illuminated from graphene and ITO sides are 1.98% and 1.95%, respectively. The open circuit voltage is about 40 mV higher than those of the devices without Au-doping, which can be attributed to the increase of the work function of the graphene electrode doped with Au, as shown in Figure 2d.

The third step is to dope graphene film with PEDOT:PSS aqueous solution in the organic solar cell to decrease the sheet resistance of the graphene electrode. Figure 4a shows the fabrication of the devices with two approaches. The first is to transfer graphene on PEDOT:PSS film as described above. The second approach is to transfer graphene on the P3HT:PCBM active layer of a device and then doped with PEDOT:PSS aqueous solution. It is noteworthy that a thin poly(methyl methacrylate) (PMMA) layer (thickness: ~0.5 μm) is spin-coated on top of the single-layer graphene film before the transfer process. So it is the graphene/PMMA film that is actually transferred on the active layer of an organic solar cell and graphene is in contact with the active layer.[17] Then PEDOT:PSS aqueous solution is dropped on the P3HT:PCBM film beside graphene/PMMA film. Since graphene is hydrophobic while P3HT:PCBM is hydrophilic after certain treatment, PEDOT:PSS solution will be adsorbed on the P3HT:PCBM layer and float graphene/PMMA film on the top. Then the device is spun on a spin coater to obtain a very thin PEDOT:PSS interfacial layer. We find that the graphene/PMMA film does not show obvious degradation of conductance after the spin-coating process even at the speed of 8000 rpm. Both graphene electrodes with and without Au-doping are used in this step. The detailed processing conditions are shown in the experimental part.

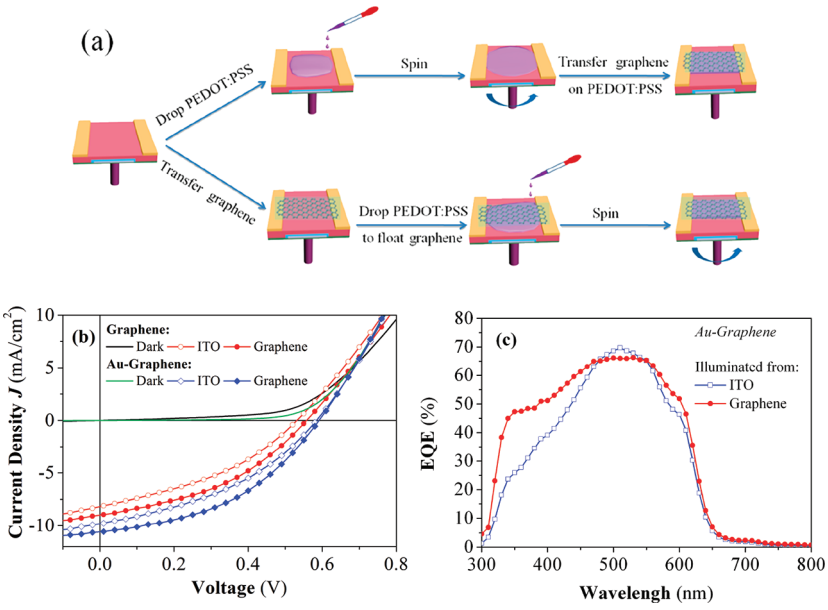

Figure 4. (a) Schematic diagram of the two approaches for the fabrication of graphene/PEDOT:PSS top electrodes in organic solar cells. (b) *J*–*V* characteristics measured from both sides of semitransparent organic solar cells with pristine or Au-doped graphene top electrode under solar simulator. Dark currents of the devices are presented as well. (c) EQE measured from both sides of the organic solar cell with Au-doped graphene/PEDOT:PSS top electrode. The open and solid symbols correspond to the results characterized from ITO and graphene sides, respectively.

TABLE 2. Photovoltaic Parameters of Semitransparent Organic Solar Cells with Different Graphene Anodes and Same ITO Cathodes

anode	illumination side	J_{SC} (mA/cm^2)	V_{OC} (V)	R_s (Ωcm^2)	FF (%)	PCE η (%)	average PCE[a] η (%)
graphene/PEDOT:PSS	ITO	8.15	0.53	21.81	37.7	1.63	1.60 ± 0.18
	graphene	9.08	0.56	21.81	39.6	2.02	2.01 ± 0.25
Au–graphene/PEDOT:PSS	ITO	9.79	0.58	12.21	39.1	2.22	2.12 ± 0.22
	graphene	10.58	0.59	12.21	43.3	2.70	2.60 ± 0.15
Au–graphene/PEDOT:PSS (after 6 months)	ITO	9.01	0.590	13.53	38.2	2.03	
	graphene	9.66	0.612	13.53	44.15	2.61	

[a] Average PCE is calculated from three devices fabricated at identical condition.

The sheet resistances of the graphene/PEDOT:PSS electrodes prepared with the two approaches are then characterized (see Supporting Information Table S1). The Au and PEDOT:PSS codoped graphene electrode shows the resistance of 152 and 96 Ω/□ before and after thermal annealing at 120 °C for 20 min, respectively. The sheet resistance is increased slightly to 105 Ω/□ after the device packaging. Compared with the pristine graphene transferred on the dry PEDOT:PSS layer, the Au and PEDOT:PSS codoped graphene electrode has the sheet resistance decreased for 80%, corresponding to the increase of the conductance for 400%, which is similar to the results observed in the graphene transistors as shown in Figure 1d. In addition, the transparency of the graphene/PEDOT:PSS electrode is up to 92% in the visible region shown in Figure 1b, which is better than multilayer graphene films used in organic solar cells before.[5,9]

The *J*–*V* characteristics and EQEs of the devices prepared by the second approach are shown in Figure 4b,c. The two devices with graphene or a Au-doped graphene electrode were characterized under a solar simulator from both sides. It is noteworthy that all of the photovoltaic parameters of the devices, as shown in Table 2, are dramatically improved after the PEDOT:PSS doping. The device with the Au and PEDOT:PSS codoped graphene electrode shows the maximum PCE (2.7%) when it is illuminated from the graphene side, which is much higher than the value from the ITO side (2.2%). The different efficiencies measured from the two sides can be attributed to the different transparency spectra of the two electrodes as shown in Figure 1b. The fill factor is improved to 43.3% due to the decreased sheet resistance of the graphene electrode. In addition, we can find that the open circuit voltage is increased for about 20 mV on average after PEDOT:PSS doping, which can be attributed to the increase of the work function of the graphene electrode, as shown in Figure 2d. The organic solar cell is very stable after it was packaged (see Supporting Information, Figure S3).

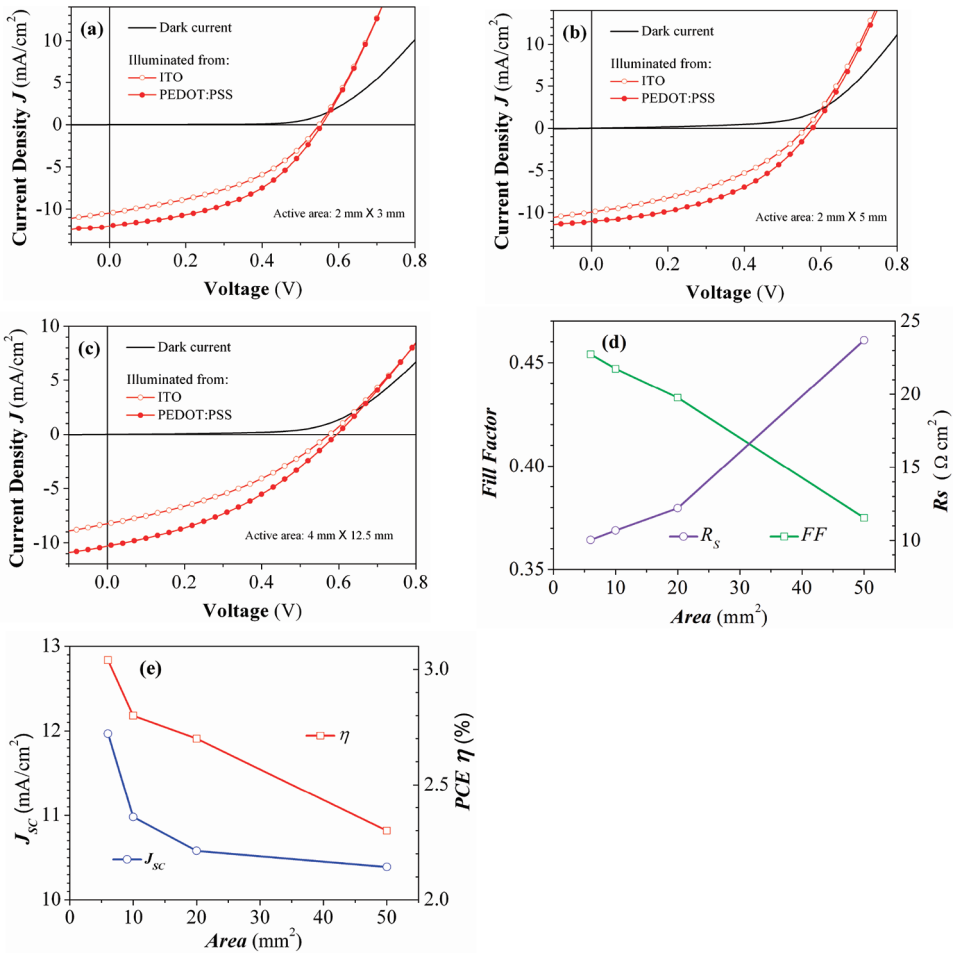

Figure 5. *J*–*V* characteristics of semitransparent organic solar cells measured under solar simulator from both sides with different active areas: (a) 6, (b) 10, (c) 50 mm^2. Dark currents of the devices are presented as well. (d,e) Photovoltaic parameters, including fill factor (FF), series resistance (R_s), short circuit current (J_{SC}) and PCE (η) of the organic solar cells with different active areas illuminated from graphene electrodes.

As shown in Table 2, the device shows very little change in efficiency after 6 months. Although J_{SC} is decreased for about several percent, V_{OC} and FF are increased a little bit.

The areas of the reported organic solar cells with graphene electrodes are relatively small ($\leq$10 mm^2), which will induce the overestimation of PCE due to the edge effect.[16] Therefore we fabricated the devices with different active areas, including 6, 10, 20, and 50 mm^2. Figure 5 panels a–c show the *J*–*V* characteristics of the devices with different sizes. Figure 5 panels d and e show the short circuit current (J_{SC}), fill factor (*FF*), series resistance (R_s) and PCE (η) of the devices. We can find that all photovoltaic parameters degrade with the increase of device area. The decrease of J_{SC} can be attributed to the less edge effect of the device with bigger size.[16] So the edge effect is negligible when the device size is bigger than 20 mm^2, which is consistent with conclusions in literatures.[16] On the other hand, the decrease of the fill factor with the increase of the device size is due to the increase of the electrode resistance and series resistance of the devices, as shown in Figure 5d and Table 3. So a graphene electrode with better conductance is needed if we want to fabricate high-efficiency organic solar cells with bigger size.

TABLE 3. Photovoltaic Parameters of Semitransparent Organic Solar Cells with Different Active Areas

active area (mmxmm)	illumination side	J_{SC} (mA/cm^2)	V_{OC} (V)	R_s (Ωcm^2)	FF (%)	η (%)
2 × 3	ITO	10.46	0.55	10.12	42.1	2.42
	graphene	11.97	0.56	10.04	45.4	3.04
2 × 5	ITO	9.93	0.56	10.98	39.4	2.19
	graphene	10.98	0.57	10.69	44.7	2.80
4 × 5	ITO	9.79	0.58	12.21	39.1	2.22
	graphene	10.58	0.59	12.21	43.3	2.70
4 × 12.5	ITO	8.33	0.58	25.50	35.6	1.72
	graphene	10.39	0.59	23.70	37.5	2.30

The efficiency of the device would be further improved if a graphene layer with a better quality was used in the devices. Bae *et al.* reported roll-to-roll production of single-layer CVD graphene film with the resistance of only 125 Ω/□.[37] It is expected that the resistance can

be decreased to a much lower value after the treatment of $HAuCl_4$ and PEDOT:PSS solution as shown in this paper. On the other hand, organic solar cells have been developed very fast and a PCE up to 7.4% has been reported recently.[38] Therefore semitransparent organic solar cells are expected to have much higher efficiency when some novel organic semiconductors and high quality graphene used in the devices.

SUMMARY AND CONCLUSION

Semitransparent inverted organic solar cells based on P3HT:PCBM were fabricated with single-layer graphene as the top electrode. The conductance of the graphene electrode was improved by doping the graphene film with Au nanoparticles and PEDOT:PSS, which resulted in an increase of conductance for more than 400%. The performance of the organic solar cell was optimized by using the doped graphene electrode and the efficiency up to 2.7% was obtained in the devices with the area of 20 mm^2. Both the efficiency and the active area of the devices are much better than the reported results for the organic solar cells with graphene electrodes. Then the effect of active area on the device performance was studied. We found that the efficiency decreased with the increase of the active area due to the increased series resistance and the decreased edge effect in the device. In addition, it is interesting to find that the semitransparent organic solar cell showed higher efficiency illuminated from graphene than from ITO side due to better transmittance of the graphene electrode. It is expected that organic solar cells with higher efficiency can be realized by using single-layer graphene with better quality and at more optimized processing conditions.

METHODS

Graphene Treatment. Graphene films were fabricated in a thermal CVD furnace using copper foils as substrates.[16] A thin layer (300 nm) of poly(methyl methacrylate) (PMMA) was spin-coated on the Cu foil and then the foil was annealed at 100 °C for about 30 min. Subsequently, the foil was put in an aqueous solution of iron chloride at room temperature. After 2 h, Cu underneath the graphene/PMMA was etched away and a visible thin film was floated on the surface of the solution. The graphene/PMMA film was then transferred to distilled water. Next, a substrate was placed in the water underneath the floating thin film to get the PMMA/graphene layer adhered to the surface of the substrate. Then the sample was taken out of water and dried for several minutes followed by the treatment of acetone to remove the PMMA on top of the graphene film. For Au doping process, graphene/PMMA film in distilled water was transferred to 2 mM $HAuCl_4$ aqueous solution at 80 °C for certain period of time. After that, the film was transferred back to distilled water and then to a substrate.

Graphene films were characterized using transmission electron microscopy (TEM, JEOL JEM-2010) and Raman spectroscopy (HORIBA JOBIN YVON, HR800). The surface potential of graphene films treated at different conditions was characterized by using scanning Kelvin probe microscopy (SKPM, Nano-Scope IV, Digital Instruments). A thin Au electrode was evaporated on part of each graphene film through a shadow mask to provide a reference of work function in the measurement. Then the surface potential of the film was scanned continuously from graphene to Au film by SKPM. Due to the different surface potentials of Au and graphene film, a potential step can be observed across the edge of the Au electrode. Since the work function of Au is 5 eV in any sample, the surface potential of graphene treated at different conditions can be calculated.

The sheet resistance of graphene film was characterized by measuring the resistance between two parallel Au electrodes in contact with graphene film, as shown in Figure 2 panels a and c. The distance between the two Au electrodes is L and the width of the graphene film is W. The resistance of the graphene film between the two parallel Au electrodes is: $R = R_{sheet}L/W$. So the sheet resistance can be calculated by: $R_{sheet} = RW/L$.

Device Fabrication and Characterization. The organic solar cells were fabricated on patterned ITO/glass substrates with sheet resistance of 15 Ω/□. The precleaned ITO substrates were treated with plasma prior to the spin-coating of ZnO precursor solution consisting of 0.5 M zinc acetate dehydrate in 2-methoxyethanol at 3000 rpm for 30 s. Then the samples were annealed on hot plate at 200 °C for 30 min in ambient air. P3HT:PCBM (weight ratio 1:0.8) dissolved in chlorobenzene with certain concentration was spin-coated onto the ZnO layer. Then the samples were annealed at 130 °C for 10 min in a N_2-filled glovebox. Au (thickness, 100 nm) films were then evaporated beside the ITO electrodes, where P3HT:PCBM film was wiped off. It is notable that the Au films were helpful in graphene transfer and device characterization. Then the graphene top electrodes were transferred on the active layer. For graphene transfer, the following two approaches were used:

(1) PEDOT:PSS was spun onto the active layer and annealed at 120 °C for 10 min. A graphene/PMMA film was picked up on the PEDOT:PSS layer and annealed in the glovebox at 120 °C for 20 min to evaporate water and improve the contact between PEDOT:PSS and graphene.[32]

(2) A graphene/PMMA film was transferred on the active layer, then PEDOT:PSS solution was dropped on the active layer beside graphene/PMMA to float the graphene film followed by spin-coating at the 3000 rpm for 30 s. After that, the device was annealed in the glovebox at 120 °C for 20 min to evaporate water and enhance the contact between PEDOT:PSS and graphene.[32] In the end, all devices were encapsulated by glass caps and epoxy in the glovebox for measurements.

The transmittance spectra of ZnO/ITO and graphene/PEDOT:PSS electrodes and semitransparent solar cells were measured by using a UV−vis spectrophotometer (UV-2550, Shimadzu, Japan). The $J-V$ characteristics of the organic solar cells were measured by using a Keithley 2400 source meter under illumination of 100 mW/cm^2 (Newport 91160, 300 W, solar simulator equipped with an AM 1.5 filter). The light intensity was calibrated with a standard silicon solar cell. The external quantum efficiency (EQE) of the devices were measured with a standard system equipped with a xenon lamp (Oriel 66902, 300 W), a monochromator (Newport 66902), a Si detector (Oriel 76175_71580), and a dual channel power meter (Newport 2931_C).

The graphene transistors were fabricated on n+Si/SiO_2 substrates. The thickness of SiO_2 was 300 nm. The channel width and length are 2.0 mm and 0.2 mm, respectively. The transfer characteristics of the graphene transistors were measured in a glovebox with a semiconductor parameter analyzer (Agilent 4156C).

Acknowledgment. This work is financially supported by the Research Grants Council (RGC) of Hong Kong, China (Project No. PolyU5322/10E) and the Hong Kong Polytechnic University (Project No. J-BB9S and 1-ZV8N)

Supporting Information Available: Figures: Raman spectrum of a single-layer graphene; light absorbance spectra of semitransparent

solar cells; *J*−*V* characteristics of an organic solar cell measured before and after six months. Tables: Sheet resistance of graphene/PEDOT:PSS electrodes. This material is available free of charge *via* the Internet at http://pubs.acs.org.http://pubs.acs.org.

REFERENCES AND NOTES

1. Novoselov, K. S.; Geim, A. K.; Morozov, S. V.; Jiang, D.; Zhang, Y.; Dubonos, S. V.; Grigorieva, I. V.; Firsov, A. A. Electric Field Effect in Atomically Thin Carbon Films. *Science* **2004**, *306*, 666–669.
2. Zhang, Y.; Tan, Y.-W.; Stormer, H. L.; Kim, P. Experimental Observation of the Quantum Hall Effect and Berry's Phase in Graphene. *Nature* **2005**, *438*, 201–204.
3. Geim, A. K. Graphene: Status and Prospects. *Science* **2009**, *324*, 1530–1534.
4. Bolotin, K. I.; Sikes, K. J.; Jiang, Z.; Klima, M.; Fudenberg, G.; Hone, J.; Kim, P.; Stormer, H. L. Ultrahigh Electron Mobility in Suspended Graphene. *Solid State Commun.* **2008**, *146*, 351–355.
5. Arco, L. G. D.; Zhang, Y.; Schlenker, C. W.; Ryu, K.; Thompson, M. E.; Zhou, C. W. Continuous, Highly Flexible, and Transparent Graphene Films by Chemical Vapor Deposition for Organic Photovoltaics. *ACS Nano* **2010**, *4*, 2865–2873.
6. Liu, J.; Yin, Z.; Cao, X.; Zhao, F.; Ling, A.; Xie, L.; Fan, Q. L.; Boey, F.; Zhang, H.; Huang, W. Bulk Heterojunction Polymer Memory Devices with Reduced Graphene Oxide as Electrodes. *ACS Nano* **2010**, *4*, 3987–3992.
7. Park, H.; Rowehl, J. A.; Kim, K. K.; Bulovic, V.; Kong, J. Doped Graphene Electrodes for Organic Solar Cells. *Nanotechnology* **2010**, *21*), 1–6.
8. Wang, Y.; Chen, X.; Zhong, Y.; Zhu, F.; Loh, K. P. Large Area, Continuous Few-Layered Graphene as Anode in Organic Photovoltaic Devices. *Appl. Phys. Lett.* **2009**, *95*), 1–3.
9. Wang, Y.; Tong, S. W.; Xu, X. F.; Özyilmaz, B.; Loh, K. P. Interface Engineering of Layer-by-Layer Stacked Graphene Anodes for High-Performance Organic Solar Cells. *Adv. Mater.* **2011**, *23*, 1514–1518.
10. Chang, H. X.; Sun, Z. H.; Ho, K. Y. F.; Tao, X. M.; Yan, F.; Kwok, W. M.; Zheng, Z. J. Highly Sensitive Ultraviolet Sensor Based on Facile *in Situ* Solution-Grown ZnO Nanorod/Graphene Heterostructure. *Nanoscale* **2011**, *3*, 258–264.
11. Lee, S.; Jo, G.; Kang, S. J.; Wang, G.; Choe, M.; Park, W.; Kim, D. Y.; Kahng, Y. H.; Lee, T. Enhanced Charge Injection in Pentacene Field-Effect Transistors with Graphene Electrodes. *Adv. Mater.* **2011**, *23*, 100–105.
12. Shi, Y.; Kim, K. K.; Reina, A.; Hofmann, M.; Li, L. J.; Kong, J. Work Function Engineering of Graphene Electrode *via* Chemical Doping. *ACS Nano* **2010**, *4*, 2689–2694.
13. Chang, H.; Sun, Z.; Yuan, Q.; Ding, F.; Tao, X.; Yan, F.; Zheng, Z. Thin Film Field-Effect Phototransistors from Bandgap-Tunable, Solution-Processed, Few-Layer Reduced Graphene Oxide Films. *Adv. Mater.* **2010**, *22*, 4872–4876.
14. Li, G.; Shrotriya, V.; Huang, J. S.; Yao, Y.; Moriarty, T.; Emery, K.; Yang, Y. High-Efficiency Solution Processable Polymer Photovoltaic Cells by Self-Organization of Polymer Blends. *Nat. Mater.* **2005**, *4*, 864–868.
15. Tai, Q. D.; Li, J. H.; Liu, Z. K.; Sun, Z. H.; Zhao, X. Z.; Yan, F. Enhanced Photovoltaic Performance of Polymer Solar Cells by Adding Fullerene End-Capped Polyethylene Glycol. *J. Mater. Chem.* **2011**, *21*, 6848–6853.
16. Cravino, A.; Schilinsky, P.; Brabec, C. J. Characterization of Organic Solar Cell: The Importance of Device Layout. *Adv. Funct. Mater.* **2007**, *17*, 3906.
17. Li, X.; Cai, W. W.; An, J.; Kim, S.; Nah, J.; Yang, D.; Piner, R.; Velamakanni, A.; Jung, I.; Tutuc, E.; Banerjee, S. K.; Colombo, L.; Ruoff, R. S. Large-Area Synthesis of High-Quality and Uniform Graphene Films on Copper Foils. *Science* **2009**, *324*, 1312–1314.
18. Ameri, T.; Dennler, G.; Waldauf, C.; Azimi, H.; Seemann, A.; Forberich, K.; Hauch, J.; Scharber, M.; Hingerl, K.; Brabec, C. J. Fabrication, Optical Modeling, and Color Characterization of Semitransparent Bulk-Heterojunction Organic Solar Cells in an Inverted Structure. *Adv. Funct. Mater.* **2010**, *20*, 1592–1598.
19. Kim, J. Y.; Lee, K.; Coates, N. E.; Moses, D.; Nguyen, T. Q.; Dante, M.; Heeger, A. J. Efficient Tandem Polymer Solar Cells Fabricated by All-Solution Processing. *Science* **2007**, *317*, 222–225.
20. Lunt, R. R.; Bulovic, V. Transparent, Near-Infrared Organic Photovoltaic Solar Cells for Window and Energy-Scavenging Applications. *Appl. Phys. Lett.* **2011**, *98*), 1–3.
21. Xia, X.; Wang, S.; Jia, Y.; Bian, A.; Wu, D.; Zhang, L.; Cao, A.; Huang, C. Infrared-Transparent Polymer Solar Cells. *J. Mater. Chem.* **2010**, *20*, 8478–8482.
22. Huang, J. S.; Gang, L.; Yang, Y. A Semitransparent Plastic Solar Cell Fabricated by a Lamination Process. *Adv. Mater.* **2008**, *20*, 415–419.
23. Mattevi, C.; Kim, H.; Chhowalla, M. A Review of Chemical Vapour Deposition of Graphene on Copper. *J. Mater. Chem.* **2011**, *21*, 3324–3334.
24. Huang, P. Y.; Ruiz-Vargas, C. S.; Zande, A. M.; Whitney, W. S.; Levendorf, M. P.; Kevek, J. W.; Garg, S.; Alden, J. S.; Hustedt, C. J.; Zhu, Y.; *et al*. D. A. Grains and Grain Boundaries in Single-Layer Graphene Atomic Patchwork Quilts. *Nature* **2011**, *469*, 389–393.
25. Tamai, T.; Watanabe, M.; Hatanaka, Y.; Tsujiwaki, H.; Nishioka, N.; Matsukawa, K. Formation of Metal Nanoparticles on the Surface of Polymer Particles Incorporating Polysilane by UV Irradiation. *Langmuir* **2008**, *24*, 14203–14208.
26. Lin, P.; Yan, F.; Yu, J. J.; Chan, H. L. W.; Yang, M. The Application of Organic Electrochemical Transistors in Cell-Based Biosensors. *Adv. Mater.* **2010**, *22*, 3655–3660.
27. Nardes, A. M.; Kemerink, M.; Kok, M. M.; Vinken, E.; Maturova, K.; Janssen, R. A. J. Conductivity, Work Function, and Environmental Stability of PEDOT:PSS Thin Films Treated with Sorbitol. *Org. Electron.* **2008**, *9*, 727–734.
28. Wu, S. J.; Tai, Q. D.; Yan, F. Hybrid Photovoltaic Devices Based on Poly(3-hexylthiophene) and Ordered Electrospun ZnO Nanofibers. *J. Phys. Chem. C* **2010**, *114*, 6197–6200.
29. Kim, J. Y.; Kim, S. H.; Lee, H. H.; Lee, K.; Ma, W. L.; Gong, X.; Heeger, A. J. New Architecture for High-Efficiency Polymer Photovoltaic Cells Using Solution-Based Titanium Oxide as an Optical Spacer. *Adv. Mater.* **2006**, *18*, 572–576.
30. Hsieh, C. H.; Cheng, Y. J.; Li, P. J.; Chen, C. H.; Dubosc, M.; Liang, R. M.; Hsu, C. S. Highly Efficient and Stable Inverted Polymer Solar Cells Integrated with a Cross-Linked Fullerene Material as an Interlayer. *J. Am. Chem. Soc.* **2010**, *132*, 4887–4893.
31. Tai, Q. D.; Zhao, X. Z.; Yan, F. Hybrid Solar Cells based on Poly(3-hexylthiophene) and Electrospun TiO_2 Nanofibers with Effective Interface Modification. *J. Mater. Chem.* **2010**, *20*, 7366–7371.
32. Wu, S. J.; Li, J. H.; Tai, Q. D.; Yan, F. Investigation of High-Performance Air-Processed Poly(3-hexylthiophene)/Methanofullerene Bulk-Heterojunction Solar Cells. *J. Phys. Chem. C* **2010**, *114*, 21873–21877.
33. Sun, Z. H.; Li, J. H.; Liu, C. M.; Yang, S. H.; Yan, F. Enhancement of Hole Mobility of Poly(3-hexylthiophene) Induced by Titania Nanorods in Composite Films. *Adv. Mater.* **2011**, *23*, 3648–3652.
34. Liu, Z. K.; Yan, F. Photovoltaic Effect of $BiFeO_3$/Poly(3-hexylthiophene) Heterojunction. *Phys. Status Solidi RRL* **2011**, *5*, 367–369.
35. Bürgi, L.; Sirringhaus, H.; Friend, R. H. Noncontact Potentiometry of Polymer Field-Effect Transistors. *Appl. Phys. Lett.* **2002**, *80*, 2913–2915.
36. Duffie, J. A.; Beckman, W. A. *Solar Engineering of Thermal Processes*; John Wiley & Sons Inc.: New York, 2006.
37. Bae, S. K.; Kim, H. K.; Lee, Y. B.; Xu, X. B.; Park, J. S.; Zheng, Y.; Balakrishnan, J.; Lei, T.; Kim, H. R.; Song, Y. L.; . Roll-to-Roll Production of 30-Inch Graphene Films for Transparent Electrodes. *Nat. Nanotechnol.* **2010**, *5*, 574–578.
38. Liang, Y.; Xu, Z.; Xia, J.; Tsai, S. T.; Wu, Y.; Li, G.; Ray, C.; Yu, L. For the Bright Future—Bulk Heterojunction Polymer Solar Cells with Power Conversion Efficiency of 7.4%. *Adv. Mater.* **2010**, *22*, E135–E138.